

IN VITRO EVALUATION OF POLYMERIZATION ENERGY FOR
BULK FILL COMPOSITES

by

Rawan S. AlRasheed

Submitted to the Graduate Faculty of the School of
Dentistry in partial fulfillment of the requirements
for the degree of Master of Science in Dentistry,
Indiana University School of Dentistry, May 2016.

This thesis accepted by the faculty of the Department of Operative Dentistry, Indiana University School of Dentistry, in partial fulfillment of the requirements for the degree of Master of Science in Dentistry.

Gabriel Chu

Joseph Wallace

Bruce Matis

Jeffrey Platt
Chair of the Research Committee

Blaine N. Cook
Program Director

Date

DEDICATION

To my guardian angel, the most giving soul and the strongest person in my life,
my mother, Fawziah Almuhaya.

ACKNOWLEDGMENTS

I would like to express my genuine appreciation to my mentor, Dr. Platt, for the continuous support, his patience, motivation, and immense knowledge.

I would like to thank the rest of my committee: Drs. Wallace, Matis, Chu, and Cook, for sharing their knowledge, their insightful comments and encouragement.

My sincere thanks also go to Jennifer Eder, Grishma Patel, and Tyler Laine for their great help in the laboratory.

I am very thankful that I was fortunate to have this study supported by the Delta Dental Foundation, and also for having a scholarship from King Saud University.

Last, but not least, I would like to thank my family and friends for supporting me spiritually throughout writing this thesis and my life in general.

TABLE OF CONTENTS

Introduction.....	1
Review of Literature.....	8
Methods and Materials.....	19
Results.....	26
Figures and Tables.....	31
Discussion.....	59
Summary and Conclusion.....	67
References.....	69
Abstract.....	76
Curriculum Vitae.....	

LIST OF ILLUSTRATIONS

FIGURE 1	Photo polymerization process of visible light cured resin based composite	32
FIGURE 2	Chemical composition of commonly used monomers in resin based composite	33
FIGURE 3	A draft illustrates the parts of the composite sample	34
FIGURE 4	MARC machine and the experiment setting	34
FIGURE 5	A diagram illustrates the position of the light cure tip in relation to the top and bottom sensors	35
FIGURE 6	Delrin rings	36
FIGURE 7	Top sensor	37
FIGURE 8	Bottom sensor	37
FIGURE 9	A draft showing the positions of the Vicker's indentation	38
FIGURE 10	Illustration of the Vicker's indentation	39
FIGURE 11	Vicker's indentation of the top surface of Tetric EvoCeram bulk fill.	40
FIGURE 12	A draft of the mold used in the AFM experiment	41
FIGURE 13	A draft of a cross section of the mold used in the AFM experiment	42
FIGURE 14	Schematic force-separation curve	43
FIGURE 15	Mean irradiance at the bottom surface	44
FIGURE 16	Total Energy (J/cm ²) at the bottom surface	45
FIGURE 17	Total energy (J/cm ²) at the bottom surface. Showing the difference between materials at each depth	46
FIGURE 18	Vicker's microhardness (N/mm ²) at the top (0 mm) and at the different depths	47
FIGURE 19	Vicker's microhardness (N/mm ²) at the top (0 mm) and at the different depths	48

FIGURE 20	Reduced modulus of elasticity (GPa) at four different locations	49
FIGURE 21	Reduced modulus of elasticity (GPa) at four different locations	49
FIGURE 22	Reduced modulus of elasticity (GPa) at four different locations	50
TABLE I	The Composite material used in the study	51
TABLE II	Information about the type of organic matrix and inorganic fillers in each composite material used	52
TABLE III	the tested depths in each material	53
TABLE IV	Comparison between the materials in the total energy (J/cm ²) transmitted at each depth	54
TABLE V	Total Energy (J/cm ²) and Mean Irradiance (mW/cm ²) at each depth of each composite material	55
TABLE VI	Vicker's microhardness number VHN (\pm SD) at the top and at each depth	56
TABLE VII	General comparison between the different materials in regards to their VHN	56
TABLE VIII	The Top/bottom ratio of the VHN of each material	57-58

INTRODUCTION

Since their development in the 1960s, resin-based composites (RBC) have become a vital part of everyday dental practice. Despite technique sensitivity and the requirement of multistep procedures, half of the posterior direct restorations placed are RBC restorations.¹ Their use has increased markedly with the improvement in dental adhesive systems. Research to improve dental composites has become an integral part of the study of dental materials due to several factors, such as an increase in patient demand for esthetic treatment, and more emphasis on conservative treatment.²

The increase in applications of composite dental restorative materials mandates a thorough and deep understanding of each component of the composite, and consideration of the methods for changing each component. The composition of RBC consists mainly of three distinct phases during which an organic resin matrix and the surrounding inorganic fillers are linked together with a coupling agent. The primary components of the resin matrix are resin monomers and an initiator (catalyst) system for polymerization. Each component represents an opportunity for improvements in the overall composite and was the target of recent research.³⁻⁵

Numerous advances in RBCs have been made during the years, which include physical, mechanical and esthetic properties. These advances were achieved mainly by manipulating the fillers and the monomer, their types, and the content. One seldom-improved property of visible light cured (VLC) RBCs is the depth at which an adequate polymerization can be achieved. This is known as the depth of cure (DOC). In 1995 Caughman et al.⁶ provided guidelines for photocuring RBCs that have not been changed

for the conventional RBCs. It was reported that 280 mW/cm² is the minimal intensity necessary to adequately polymerize a 2 mm-thick increment of universal shade composite. It was also reported that increasing the intensity to 800 mW/cm² combined with an increase in the exposure time to 80 sec was not effective in adequately polymerizing the composite at a depth of 3 mm.^{6,7}

A number of methods have been used to assess the DOC in the literature. The ISO 4049 standard is the simplest method, which uses a micrometer to measure the thickness of RBC that remains after removal of uncured soft material.⁸ Other methods involve measurement of the degree of conversion (DC) using Raman or FTIR spectroscopy – or of the microhardness (MH)⁹ at consistent intervals throughout the depth of the material. Based upon these measurements, the DOC is described as the depth at which the MH or DC value equals the surface value multiplied by an arbitrary ratio, usually 0.8.¹⁰

Since RBCs are composed of organic matrix and fillers as mentioned previously, there is a significant need to develop a technique differentiating the properties of the organic matrix and the fillers' impact on the material properties.⁴ It must be mentioned that the quality of polymerization is primarily linked to the resin phase of the material, which consists 30 volume percent to 40 volume percent of the RBCs. In other words, most of the material is composed of fillers, which are tightly packed, leaving very little space for the resin between them. For example, the width of the indentation left by a Vickers indenter in a dental RBC is around 60 μm . This is considerably larger than the distance between two neighboring filler particles that the resin occupies, which is found to be less than 1 μm based on scanning electron microscopy (SEM) images.^{11,12} Recently, several analytical techniques have been developed, or newly applied to help characterize

RBCs. A nanoindentation technique was used to obtain the localized hardness and elastic modulus, and to assess the viscoelastic response based on a progressive-load scratch test.⁴

J.G. Leprince et al. in 2012 proposed revising the definition of DOC, taking into consideration the point where the resin-matrix shifts from a glassy to a rubbery state. They suggested that the properties currently used to evaluate depth of cure (microhardness, degree of conversion, or scraping methods) fail to detect this transition, resulting in overestimation of the depth of cure. A specific technique was used to highlight this transition, i.e. atomic force microscopy (AFM), to measure the elastic modulus of the resin between the fillers (E-Mod, MPa).¹¹

It is crucial to dental practitioners to have knowledge of the maximum thickness at which an adequate polymerization of RBCs is achieved. Insufficient polymerization of RBCs is known to affect the mechanical, physical, and esthetic properties of RBCs, and their biocompatibility, including reduced biocompatibility due to elution of residual monomer,¹³ reduced color stability, increased solubility, and increased water sorption.¹⁴

Optimizing RBC polymerization has been the aim of many researchers, who have tried to achieve it with different approaches. One of these approaches is “the incremental layering technique.” This is controlling the maximum thickness of the resin composite increment during its application to ensure bottom surface polymerization. Many studies have suggested 2 mm as the maximum thickness of RBC increments.^{6,7,15} In addition to ensuring adequate resin polymerization, this technique possesses other advantages such as reducing the stresses resulting from RBC polymerization shrinkage, which in turn supports a better marginal adaptation to the cavity walls and/or margins with less cuspal distortion.^{16,17} On the other hand, this technique is sensitive, time consuming, and

involves a higher risk of incorporating air bubbles or contamination between increments.¹⁸

In recent years, bulk fill RBCs have been introduced with claims of improved RBCs properties, including an increased depth of cure, up to 4-mm to 5-mm increments, with similar or even reduced polymerization shrinkage. There is also a better adaptation to cavity walls or margins due to the different rheology of the new materials. These improvements save time, reduce the technique sensitivity of the RBCs, and provide better marginal adaptation.¹⁹ However, more research is needed to carefully examine these new materials and remove concerns about using them. One major concern is the adequacy of RBC polymerization at the supposedly increased depth of cure. As stated earlier, inadequate polymerization will have a negative effect on the success of the RBCs. Knowing that the bulk fill RBCs are adequately cured will help to encourage dental health care professionals to include the new materials in treatment options. Increased depth of cure will eliminate the need for the time consuming 2-mm incremental layering. The depth of cure is dependent on several factors: the type of light; the type and the concentration of photoinitiators; the shade and the translucency of the restoration; the exposure time, and the distance from the light-curing source.^{9,20}

Deeper insight about the polymerization of bulk filling materials was the general goal of the present study. The aims were:

1. To measure the light energy transmitted through the composite resin material at different points through its thickness, and from these data, to measure the threshold energy needed to achieve adequate polymerization.

2. To measure the microhardness at the top and bottom surfaces of the composite resin specimen using Vickers microhardness.
3. To measure the elastic modulus of the resin, at different depths, using atomic force microscopy (AFM).
4. To determine if there is a correlation between the light energy transmitted through various depths, microhardness, and elastic modulus profiles.

NULL HYPOTHESES

1. Between different products of resin composite, no difference exists regarding:
 - The depth of cure when the microhardness method is used.
 - The elastic moduli changes using the AFM method.
 - The total energy level needed to reach the adequate polymerization (i.e. the depth at which microhardness value equal at least 80 percent of the value at the top surface).
2. There is no correlation between the light energy transmitted through various depths, microhardness, and elastic modulus profiles.

ALTERNATIVE HYPOTHESES

1. Between different products of resin composite, there will be a difference in terms of depth of cure when the microhardness method is used.
2. The elastic moduli changes using the AFM method.

3. The total energy level needed to reach the adequate polymerization (i.e. the depth at which microhardness value equals at least 80 percent of the value at the top surface).
4. There is a correlation between the light energy transmitted and various depths, microhardness, and elastic modulus profiles.

REVIEW OF LITERATURE

VISIBLE LIGHT CURE RESIN BASED COMPOSITE

For more than half a century manufacturers and researchers have been striving to improve the resin based composite (RBCs) characteristics, in an attempt to find the ideal material mimicking natural tooth structure characteristics. The early (RBCs) were chemically activated. The generation after that were photo-activated composites initiated with ultraviolet (UV) wavelengths

It was not until the 1980s when the visible light cured (VLC) RBCs were introduced in the dental market.²¹ They became popular very fast and their use is increasing worldwide because of the advantages they hold over the chemically activated type, such as: giving more control over the setting time, no mixing is needed resulting in fewer voids, greater strength, better shade selection, improved color stability and higher surface polymerization than chemically activated RBCs. VLC RBC polymerization is initiated by photoinitiators (mainly camphorquinone) which absorb the light energy emitted from a curing light.^{3,5,22}

As the use of VLC (RBCs) is increasing, it has been found that patients with high-caries risk experience secondary caries more frequently in large composite restorations. The leading disadvantage of (VLC) RBCs is polymerization shrinkage, which stresses the tooth/adhesive bond. Clinically, this can lead to crack formations in dentin and enamel, sensitivity, discoloration, and secondary caries.²³ These drawbacks show a need for development and a comprehensive understanding of RBCs components.⁴ Henceforth, it is

imperative to evaluate the factors affecting photo polymerization efficiency of VLC (RBCs).

Many studies that were directed toward improvement of RBCs found that the major weakness of the material comes from inadequate polymerization. Subsequent research focused on techniques that would sufficiently assess the polymerization as well as identifying the factors that play a major role in the polymerization process.

One way that has been suggested to obtain adequate resin polymerization on the bottom surface is the “incremental layering technique,” which was described earlier in the introduction. For many years the suggested maximum thickness of an increment was 2 mm.^{6,7,15} The incremental technique possesses additional advantages such as: Providing better marginal adaptation to the cavity walls/margins achieved by reducing the stresses resulting from RBC polymerization shrinkage and reducing cuspal distortion.^{16,17} That being said, there are some disadvantages: it is time consuming, technique sensitive, and engages an increased risk of incorporating air bubbles or contaminants between increments.^{18,24,25} These shortcomings were addressed in the recent developments in the RBC. Modern advances incline towards new monomers, initiator systems, optical properties,^{26,27} and filler technology.²⁸ These recent advances ultimately led to the introduction of “bulk fill” RBCs . Manufacturers of bulk fill RBCs are promising an increased depth of cure, up to 4 mm to 5 mm per increment, without compromising other traditional VLC (RBCs) properties, such as: polymerization shrinkage and adaptation to cavity walls/margins. These improvements are advertised to be a time saver, reduce technique sensitivity and provide better marginal adaptation.

Cramer et.al 2011 suggested that advances in RBCs rely mainly on comprehensive understanding of each material component. In 2013, Leprince et.al argued that the successful placement of RBCs also depends on the efficiency of the photopolymerization process.^{4,29} Both strategies in improving RBCs are valid, and they go hand-in-hand in obtaining a better material.

This review will focus on the factors that have a role in enhancing the polymerization efficiency and the methods suggested for evaluating it.

PHOTOPOLYMERIZATION PROCESS

While reviewing the factors of polymerization efficiency of VLC (RBCs), the properties used to assess efficiency are focused on dental photopolymer technology. New monomer technological advances have been introduced to the dentistry field. The dimethacrylate-based composites (DBC) now embody the majority of materials used for direct restoration. There are many factors affecting the polymerization efficiency. Intrinsic elements include the photo initiator type, concentration, viscosity, and optical properties. Extrinsic features include light type and spectrum, curing modes, temperature and light guide tip location, and irradiation parameters.²⁹

The photo polymerization process of VLC (RBCs) is a reaction generated by irradiation of a light-sensitive initiator and the linking of methacrylate groups. The steps of this reaction are described as initiation, propagation, cross linking and termination. Leporine (2013) simplified the visualization of this process through a schematic representation (Figure 1).

A conventional measurement of the effectiveness of the polymerization is done by comparing the amount of double bonds in the final structure to the original amount. The ratio of this measurement is expressed as a percentage named the degree of conversion (DC), and the DC value is generally in the wide range of 35 percent to 77 percent.²⁹

MONOMERS

Generally speaking, the most common monomers used in the organic resin matrix are 2,2-bis [4(2-hydroxy-3-methacryloxy-propyloxy)- phenyl] propane (Bis-GMA) and urethane dimethacrylate (UDMA). Some resins contain one of these, and others may contain both. At each end, these molecules have a carbon double bond, which undergoes an addition polymerization reaction if initiated by a free radicals from the photoinitiator.³⁰

With respect to viscosity, two main factors affect the composites system: monomer composition and filler content. Differences in monomer molecular structure and proportions can affect polymerization efficiency. Bis-GMA, a part of the common mixture bis-GMA/TEGDMA, mainly controls the polymerization mechanisms and kinetics.³¹ It was found that in pure bis-GMA, the maximum polymerization rate (MPR) develops at less than 5-percent conversion because of its high viscosity. In contrast, it was found that in the pure TEGDMA, which has much lower viscosity, the MPR is observed near 22-percent conversion. The final DC of bis-GMA is about 30 percent and over 60 percent for TEGDMA.³¹ This means it can be predicted that for any new dimethacrylate monomer affecting viscosity, polymerization efficiency will be influenced as well.²⁹

Fillers also have a significant influence on polymerization efficiency. The effect of fillers within a resin is to reduce the maximum DC.³²⁻³⁴ There are significant differences in DC (48 percent to 61 percent) with constant filler volume (56.7 percent) due to differences in filler size and geometry.³⁵ Given these differences, changes in DC are possibly due to local monomer mobility, controlled by variations of the filler-resin contact region, which can produce local variations of viscosity in the resin.³⁶

PHOTOINITIATORS

Recent developments in dental resin technology include the use of different photo initiator systems with trimethylbenzoyldiphenylphosphine (TPO) and dibenzoyl germanium derivative (Ivocerin).^{37,38} Camphorquinone (CQ), the generally used photo initiator, is used in combination with a tertiary amine as a co-photoinitiator. Although TPO and Ivocerin have been employed, the emission spectrum of LED light-curing units is best used for the higher absorption wavelengths of the CQ photoinitiator (430 nm to 480 nm), while the range of TPO is 350 nm to 425 nm²⁰ and Ivocerin is 370 nm to 460 nm.³⁸ Knowing there is an absorption wavelength mismatch to be overcome, LED chips with differing yields are used in poly-wave light curing units. While the light beam of LED light-curing units may be inhomogeneous, the effect of this, with respect to depth of cure at deeper areas, can be examined by creating a complete curing profile.²⁴

DEGREE OF CONVERSION

Degree of conversion is a very important aspect due to it being highly correlated to several material characteristics. These characteristics are mechanical properties^{20,21} that include volumetric shrinkage,²² wear resistance,²³ and monomer elution.²⁴ DC is regularly measured to examine polymerization efficiency by way of spectroscopic

techniques that analyze the residual double bonds, including mid-infrared Fourier transform (FT)²⁵ or Raman spectroscopy.²⁶ When considering polymerization at different depths, mid-IR techniques use microscope attachments and fixated beams used in micro-Raman spectroscopy to measure DC at specific points and to plot the surface of the sample. One disadvantage of mid-IR methods is high absorption in the wavelength range, which may increase variability of results in testing. Newly practiced, near-infrared FT spectroscopy (FT NIR), centered around transmissions, has been shown an efficient and trustworthy method to use in real time. In addition, DC has been indirectly evaluated by microhardness measurements (Vickers, Knoop) as a linear correlation was previously observed between DC and microhardness values.^{27,29,30} While exploring the degree of crosslinking, some researchers disagree with the correlation due to factors other than DC affecting a sound microhardness measurement. As a whole, microhardness measuring will not offer quantitative data on tangible changes in the reactive groups.

DEGREE OF CROSSLINKING

In addition to DC, the degree of crosslinking is also an important determinant of mechanical properties³² and structural stability. The more swelling and degradation in solvent, the less crosslinked the material.³³⁻³⁵ As crosslinking increases, there is an indirect reaction of reduced molecular mobility, which can be emphasized by an increase in glass transition temperature (T_g). This progression can be measured by both dynamic mechanical analysis and differential scanning calorimetry. Given that T_g can offer an indication of the crosslinking density, it also relies on DC and monomer viscosity. As a result, it is challenging to differentiate the effects of factors contributing to crosslink density.

DEPTH OF CURE

The term depth of cure (DOC) generally refers to the maximum thickness of VLC (RBCs) that is adequately cured. The curing adequacy is affected by multiple factors such as the type and concentration of photo initiators,^{33,39} the type, size, and amount of fillers and their optical properties,⁴⁰ and the irradiation parameters.⁴¹

Many methods have been employed to evaluate the DOC. One of the simplest methods was explained in the ISO Standard 4049. It basically measures the remaining hard material after it has been light cured and the soft under-cured material is removed; the material DOC will be the measurement divided by two.^{8,9} The rationale for using a division factor is that not all hardened material is adequately cured.^{10,26}

Other methods include measurement of the material microhardness (MH), or the degree of conversion (DC) throughout the RBC depth.^{9,42,43} Based on this measurement, the DOC will be determined as the depth at which the surface shows a DC or MH value that equals at least 80 percent of the values measured at the top surface.¹⁰

It can be questioned whether these methods are appropriate for measuring the quality of cure of an RBC at depth; however, it is challenging to determine which DC best corresponds to adequate polymerization. On its own, the DC value is inadequate because it does not provide information related to the degree of crosslinking. A higher degree of crosslinking in dimethacrylate-based polymers creates a non-linear polymerization process. This process is shown by two macroscopic changes of state: gelation and vitrification. The gelation occurs at a relatively low DC (<10 percent) and the vitrification, known as the conversion from a rubbery to glass-like makeup, is accompanied by an increase in elastic modulus (3d to 4th order of magnitude).⁴ The

combination of DC and the degree of crosslinking determines when a polymer network gels and vitrifies, and these phases have been well documented by real-time measurement of DC in these samples (<2 mm). These samples support the conclusion that as DC and crosslinking increase with radiation time, the liquid resin will experience gelation and then vitrification.⁴⁴

A decrease in crosslinking occurs as the depth increases, with only 25-percent transmittance at 1 mm, 12 percent at 2 mm, and 7 percent at 3 mm. Furthermore, polymerization experiments have revealed it is plausible that at a certain depth, the resin could transform from glassy to rubbery, and then, from rubbery to liquid state. Of the transitions, changes between gel and liquid are easily noticeable. Conversely, the hypothetically quick transitions from rubbery to glassy polymer have yet to be described, because procedures to measure this event have yet to be developed. With regard to a disproportionate micro-indenter and what needs to be measured, it must be recognized that the quality of polymerization concerns only the resin phase of the filler, which is comprised of 30 percent to 40 percent of the most heavily filled RBCs. Additionally, the majority of the material is made of tightly packed fillers, which leaves minute space for the resin in between them. For example, the indentation left by the Vickers indenter in an RBC is close to 60 μm , which is larger than the distance between two fillers that the resin inhabits.¹² This comparison summarizes the struggles in evaluating properties of the resin using hardness, penetrometer, and scraping measurements, and suggests that other method be used.¹¹

BULK FILL COMPOSITE⁴⁵

Alshali et al. in 2013 stated that generally, the degree of conversion values of the bulk-fill composites (SureFil SDR and Venus Bulk Fill) were comparable to those of conventional composites studied. The resin chemical composition in the studied bulk fill RBCs does not seem to influence the polymerization process in a negative way.⁴⁶ A laboratory evaluation of bulk fill vs. traditional RBCs was done by Tiba et al. in 2013. They found that the laboratory performance of bulk fill RBCs is comparable to the traditional RBCs with the exception of depth of cure and Knoop hardness. Three of the tested bulk filled RBCs failed to achieve adequate depth of cure when tested according to the ISO 4049-2009 standard. SonicFill, Tetric EvoCeram and Alert condensable composite did not pass the specification. On the other hand, all products tested but one (Alert Condensable) demonstrated adequate hardness after curing.⁴⁷

On the other hand, Leprince et al. (2013) looked at the physico-mechanical properties of a few commercially available bulk fills, and they stated that the advantages that accompany this particular class of material, such as convenience and time savings, come at the expense of mechanical properties when compared with the traditional RBCs.⁴⁵

It is highly important to gain knowledge about the chemical composition and photopolymerization properties of any newly introduced material, especially because manufacturers are reluctant to reveal the actual composition of commercially available products.²⁹

Photoinitiators in bulk fill RBCs are similar to those of regular RBCs, with CQ being the most common photoinitiator compound.^{48,49} However, Ivocerin is an additional

photoinitiator used in Tetric Evoceram Bulk Fill. This latter compound is reported to have higher absorption of visible light. Hence, it has a higher activity in photo curing than CQ.³⁸

Regarding monomer composition of the bulk fill materials, Alshali et al. in 2015 found the bulk-fill RBC's matrix compositions were comparable to those of the traditional RBCs except for SureFil SDR . The main monomers revealed were BisGMA, UDMA, TEGDMA, and BisEMA. Monomers were detected in variable combinations for different materials with significant differences in their relative amounts. Other monomers were detected as well, such as: 1,6-Hexanediol di-methacrylate (HDDMA); diethylene glycol di-methacrylate (DEGDMA); Bis-(acryloyloxymethyl); tricyclo[5.2.1.0.sup.2,6]decane (TCD-DI-HEA), and (SDR-urethane dimethacrylate) SDR-UDMA in Grandioso flow, X-flow, Venus Diamond, and SureFil SD, respectively.⁵⁰

MATERIALS AND METHODS

The composite resin materials used in the present study were Tetric EvoCeram Bulk Fill (TEC), SonicFill (SF), X-tra fill (XF), and Premise (P). They are described in Table I and Table II

MARC RESIN CALIBRATOR

The Managing Accurate Resin Curing® Resin Calibrator (MARC ® RC, Bluelight Analytics, Inc.) is a relatively new machine commonly reported in the literature. The MARC enables measurement of the amount and the type of energy delivered to the top surface of resin composite specimens, and also the amount and the type of energy that passes through the bottom surface of an increment of resin composite.

Components of the resin calibrator

All optical components central to this calibrated measurement system are securely contained within an aluminum box including two cosine corrector sensors. They are 4 mm in diameter and connected to a spectrometer with a bifurcated fiber optic cable. The top sensor measures the amount, the type, and the rate of energy delivered to the top surface of a resin composite specimen. The bottom sensor measures the amount, the type, and the rate of energy transmission through a resin composite specimen. The spectrometer is a calibrated spectrometer (Ocean Optics), custom configured and optimized to measure curing lights in wavelengths between 360 nm 540 nm. The spectrometer is mounted inside the resin calibrator and is connected to the sensor using a bifurcated fiber-optic cable. The device includes a clamp to hold the curing light, a

universal adjustable arm attached to a Y-Z pinion jack and linear translation stage, with the entire unit attached to a bench plate. The assembly enables the operator to precisely control the position of the curing light over and between the sensors.

SPECIMEN FABRICATION

All procedures were performed in a light controlled (dark) room. Using acetal (Delrin®) rings (Figure 6), cylindrical specimens of 6-mm diameter and different depths (Table III) were filled with the test material according to the following procedure: The acetal ring was sprayed with dry lubricant spray and placed on a Mylar strip. The Mylar strip was secured in place with tape and supported on a glass slide to ensure a smooth surface of the resin composite. The ring was filled with the test composite resin and then another Mylar strip was placed on top. A glass slide was placed over the top Mylar strip and pressed down to obtain a flat smooth surface and to extrude excess material (Figure 3 and Figure 4).

The curing light was placed within the resin calibrator device so that it was immediately above and at 90° to the top surface sensor (Figure 5).

The specimen was placed on top of the bottom sensor and light cured. During the light curing procedure, the bottom sensor measured the amount, the type, and the rate of energy transmission through the resin composite specimen. The obtained data were analyzed to understand the correlation between the amount of light energy and the measured properties at various depths of the bulk-filled composite resin being tested.

After testing with the MARC, all specimens were stored in a dry, dark container, at room temperature, 23°C , until Vickers microhardness testing was performed 24 hours after light activation.

Vickers microhardness test: All measurements were made using the following parameters: Load: 200 g; dwelling time: 15 s; indenter: Vickers Diamond indenter. The machine used for this test was manufactured by Leco Corporation, Model: LM247AT, which uses Confident v.2.5 software.

For each sample, three VHN readings were recorded for the top (closest to the curing unit) and bottom (farthest from the curing unit) surfaces. Three points were also chosen in the middle of the sample, 1 mm right of the middle, and 1 mm left of the middle (Figure 9). Then, for each thickness, the mean value and corresponding standard deviation of the VHN were measured. Also, a bottom-to-top VH percentage was determined and a value of 80 percent was used to indicate acceptable curing.

SAMPLE FABRICATION FOR ATOMIC FORCE MICROSCOPY (AFM)

Reduced elastic modulus (E_m) was determined with atomic force microscopy (AFM) using a block-shaped and custom-made acrylic mold with a semicircular notch of 10-mm length and 4-mm diameter (Figure 12). The semicircular notch was entirely filled with one of the test resin composites. The mold was covered with a Mylar strip (Hawe Stopstrip Straight, KerrHawe) and the resin composite made flush with the mold by use of a glass slide. The Mylar strip was secured in place using tape. Excess resin material was removed. Then, the mold was covered with an acrylic shell (Figure 13). A second Mylar strip was placed on the semicircular opening and the resin was composite light-cured through the semicircular opening (top surface) for 20 s keeping the light tip centered and in contact with the second Mylar strip. After light curing, the shell and both Mylar strips were removed. The mold including the resin composite specimen was placed

in an ultrasonic machine with deionized water for 10 minutes, and then it was stored dry in a dark container in the controlled room for 48 hours before the AFM analysis.

ATOMIC FORCE MICROSCOPY (AFM) IMAGING AND INDENTATION

Each composite material was in an experimental group. Four (4) groups are indicated in Table I. Sample imaging in this test was accomplished using a Bruker Catalyst AFM, operating in peak force tapping mode using RTESPA probes (Bruker, radius nominally 8 nm, $k = 40 \text{ N/m}$).

RE-IMAGING PREPARATION

Probe calibration: The probe was pushed onto a glass surface and the deflection of the cantilever was measured to determine the cantilever's deflection sensitivity (nm/V). Next, the spring constant (N/m) of the cantilever was determined using the thermal tuning method. Finally, the radius of curvature was determined using a tip calibration sample.

Imaging

At four depths in each of four samples per experimental group, $10 \mu\text{m} \times 10 \mu\text{m}$ images were obtained (i.e. at the surface, then at 2-mm intervals).

Post-imaging

After imaging a location, a grid of 100 indentations was implemented with a maximum force of 100 nN, and force-separation curves (Figure 14) were acquired and analysed. Indentation modulus (E_s) was calculated from the unloading curve using a contact mechanics approach based on the classic Hertzian model of contact between a rigid sphere and an elastic half space:

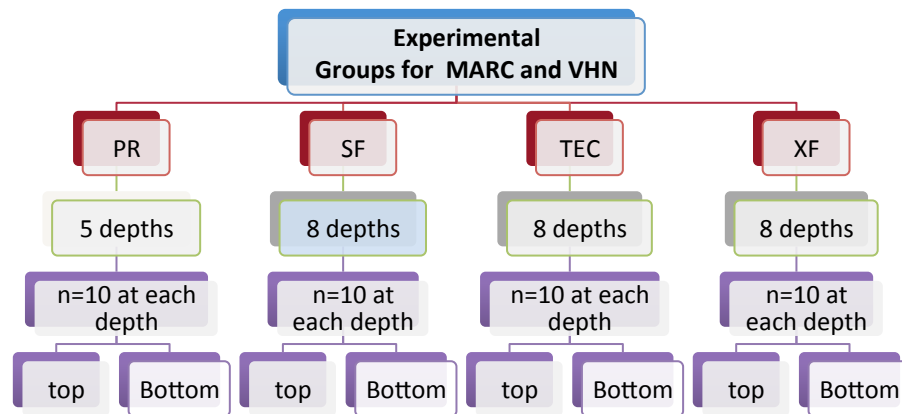
$$F = \frac{4}{3} \cdot \frac{E_s}{1 - \nu_s^2} \cdot \sqrt{r} \cdot \delta^{\frac{3}{2}} \text{ (equation 1)}$$

In equation 1, F is force and δ is deformation; r is the radius of curvature of the probe. Poisson's ratio (ν_s) is not known for these samples. It is not possible to determine ν_s as it will be different for each material as well as changing across the depth of the sample. These differences are attributed to variations in the degree of polymerization. That being said, the reduced elastic modulus (E^*) was determined using the following equation:

$$E^* = \frac{E_s}{1 - \nu_s^2}$$

STATISTICAL ANALYSIS

The effects of group, location (top, bottom), and curing depth on VHN were analyzed using mixed-model ANOVA. Elastic modulus and light energy comparisons were made using two-way ANOVA with factors for group and depth. The distributions of all measurements were examined. The MARC data were log-transformed (base 10), and analyzed with a 2-way ANOVA. The VHN data was log-transformed (base 10), and analyzed with a three-factor mixed-model ANOVA. The AFM data were log-transformed (base 10), and analyzed with a two-way mixed-model ANOVA, with a random effect for the samples within the groups. A 5-percent significance level was used for all tests.



The study had 80-percent power. A detailed sample size distribution is explained in the chart above.

RESULTS

The MARC data were log-transformed (base 10), and analyzed with a two-way ANOVA. Overall, there was a significant difference in the depths for low-mid-range energy, mid-high range energy, maximum irradiance, mean irradiance, and total energy; a significant difference in the materials for mid-high range energy, mean irradiance, and total energy; and a significant difference in low-mid range energy for the interaction of depth and material.

The light mean irradiance at the top surface ranged between 908.1 -1083.747 mW/cm² with mean of 977 ± 20.6 mW/cm², while the total energy at the top surface ranged from 19-22 J/ cm² with a mean of 20 ± 0.6 . For all tested materials, both mean irradiance and total energy decreased significantly with increasing sample depth. There was a significant difference among different materials in the net difference of total energy, except for TEC and SF. On the other hand, a significant difference in the net mean irradiance was only observed when P was compared with TEC and XF (Figure 15).

Comparing the total energy measured at the bottom surface at various depths in different materials, there was a significant difference among all materials, different depths, and the interaction between depth and material. (Figure 16 and Figure 17) (Table IV).

Since the light irradiance and total energy were measured at the bottom surface of several material thicknesses, it was possible to find out the values that correspond to depth at which VHN were 80 percent of the surface value. For example, at the depth of 3 mm of Premise material, the mean irradiance measured at the bottom was as low as

53.72±3.17 mW/cm² while the total energy was 0.84± 0.12 J/cm². Considering other materials, the total energy varied between different materials, (0.31±0.17, 0.52±0.02, 0.56±0.02) for SF, TEC and XF respectively. More details are shown in Table V.

Vickers's Microhardness (VHN)

The VHN data were log-transformed (base 10), and analyzed with a three factor mixed-model ANOVA, with a random effect to get the correlation between the bottom and top. Overall, there was a significant difference in VHN for the different materials, depths, locations, and their interactions. X-tra fill VHN was the highest compared with other materials regardless of the depth, with mean VHN =86.4 ± 1.8 at the top surface. On the other hand, TEC VHN showed the lowest score with a mean of 48.86 ± 2.9 at the top surface. All tested materials showed a significant gradual decrease in the VHN as the depth increases (Table VI). There was a significant difference in the VHN between all the materials at each depth ($p < 0.001$), except between P and TEC at 4 mm and between SF and TEC at 7 mm (Figure 18 and Figure 19).

The ratio of bottom to top was calculated from the VHN data, then the ratio data were log transformed (base 10) and analyzed with a 2-way ANOVA.

Overall, there was a significant difference in the Vicker's microhardness (bottom:top) ratio for different materials and depths, and there was a significant interaction among material and depth ($p < 0.0001$) (Table VII). XF showed the largest depth of cure of 7 mm and P was the lowest with depth of 3 mm. It was 5 mm and 6 mm for SF and TEC, respectively. All four materials met the manufacturers' claims regarding their depth of cure when the manufacturer's instructions were followed (Table VIII).

AFM

The AFM data were log-transformed (base 10), and analyzed with a 2-way mixed-model ANOVA, with a random effect for the samples within the groups. Overall, there was a significant difference in elastic modulus for the different materials, locations, and the interaction of material and location.

Looking at the effect of the material, there was a significant difference in the reduced elastic modulus across the various depths of the samples. Premise had a significantly lower reduced elastic modulus than SonicFill, Tetric EvoCeram, and X-tra Fill. SonicFill had a significantly smaller elastic modulus than Tetric EvoCeram Bulk Fill and X-tra fill. X-tra fill had a significantly smaller elastic modulus than Tetric EvoCeram Bulk Fill (Figure 6), $\text{Premise} < \text{SonicFill} < \text{X-tra fill} < \text{Tetric EvoCeram}$.

In general, there was a significant difference in the reduced elastic modulus at the different locations. Location 4 had a significantly smaller elastic modulus than locations 1, 2, and 3. Location 3 has a significantly smaller elastic modulus than Locations 1 and 2. Locations 1 and 2 were not significantly different (Figure 20, Figure 21).

$\text{Location 4} < \text{Location 3} < \text{Location (1, 2)}$

The interaction between the location and the material effects resulted in different outcomes in different materials tested. The reduced elastic modulus was significantly different in each location from the other for Premise. The reduced elastic modulus was significantly different as the depth increased (Figure 22). On the other hand, the reduced elastic modulus of Tetric EvoCeram Bulk Fill showed no significant difference among the different locations across the depth of the sample. In Sonic Fill, location 3 was significantly less than the other tested locations. Xtrafill showed that reduced elastic

modulus reduction in location 4 was significantly different from locations 1 and 2, but not location 3; the latter showed no significant difference than the other locations.

FIGURES AND TABLES

FIGURE 1. Photo polymerization process of visible light cured resin based composite. Adapted from 11: Leprince, J.G., et al., New insight into the "depth of cure" of dimethacrylate-based dental composites. Dent Mater 2012;28(5):512-20.

FIGURE 2. | Composition of commonly used monomers in resin based composite.
Adapted from Powers, Sakaguchi, and Craig.⁵

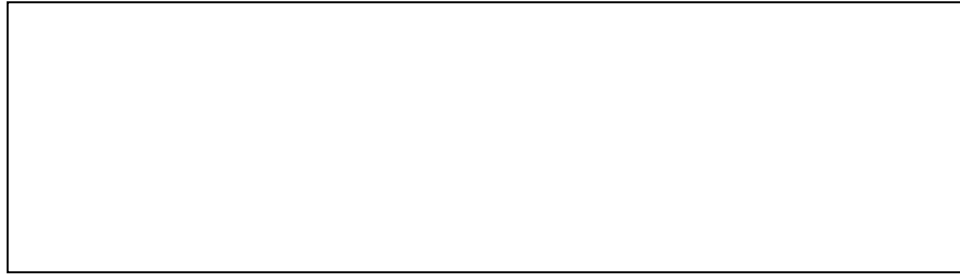


FIGURE 3. A draft illustrates the parts of the composite sample.

FIGURE 4. MARC machine and the experiment setting.

FIGURE 5. A diagram illustrates the position of the light cure tip in relation to the top and bottom sensors during the experiment.

FIGURE 6. Delrin rings.

FIGURE 7. Top sensor.

FIGURE 8. Bottom sensor.

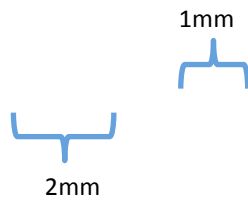


FIGURE 9. A draft showing the positions of the Vicker's indentation, the space between indentations is 1 mm, and the space between an indentation and an edge is 2 mm.

FIGURE 10. Illustration of the Vicker's indentation. Adapted from Powers, JM, Sakaguchi RL, Craig RG. Craig's restorative dental materials. 12th ed. St. Louis, Mo.: Mosby Elsevier, 2006; xvii, 632 p.⁵

FIGURE 11. Vicker's indentation of the top surface of Tetric EvoCeram Bulk Fill.

FIGURE 12. A draft of the mold used in the AFM experiment showing the placement of the composite material.

FIGURE 13. A draft of a cross section of the mold used in the AFM experiment.

FIGURE 14. Schematic force-separation curve. Adapted from AD Kemp et al. *J Structural Biol* 2012;180:428–38.⁵¹

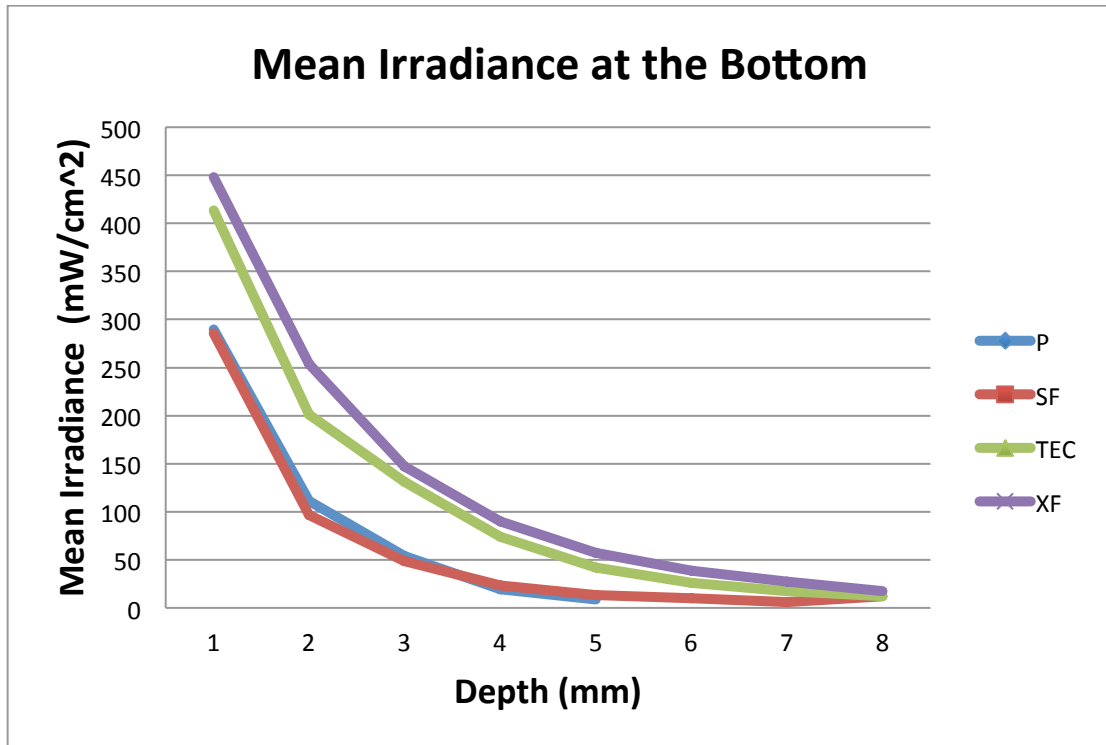


FIGURE 15. Mean irradiance at the bottom surface.

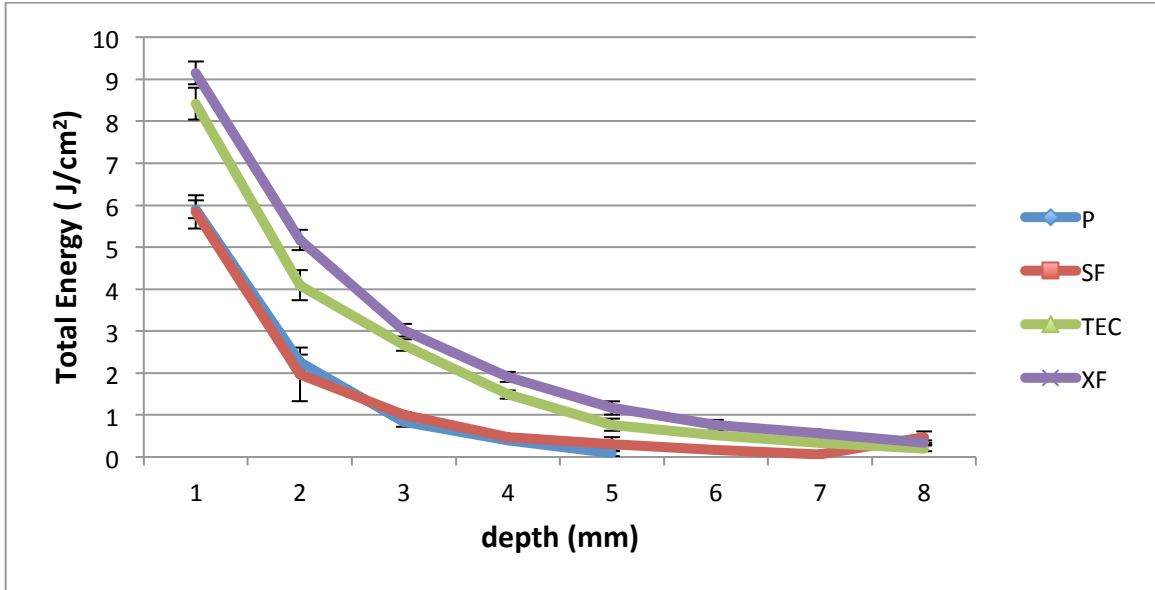


FIGURE 16. Total Energy (J/cm²) at the bottom surface.

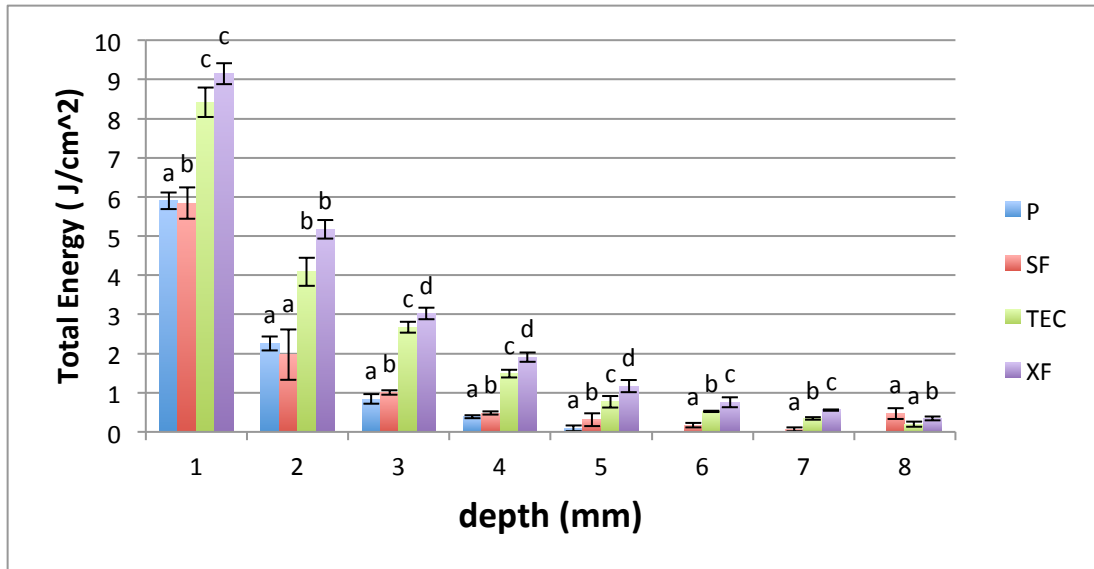


FIGURE 17. Total energy (J/cm²) at the bottom surface. Showing the differences between materials at each depth.*Materials with the same letter are not significantly different.

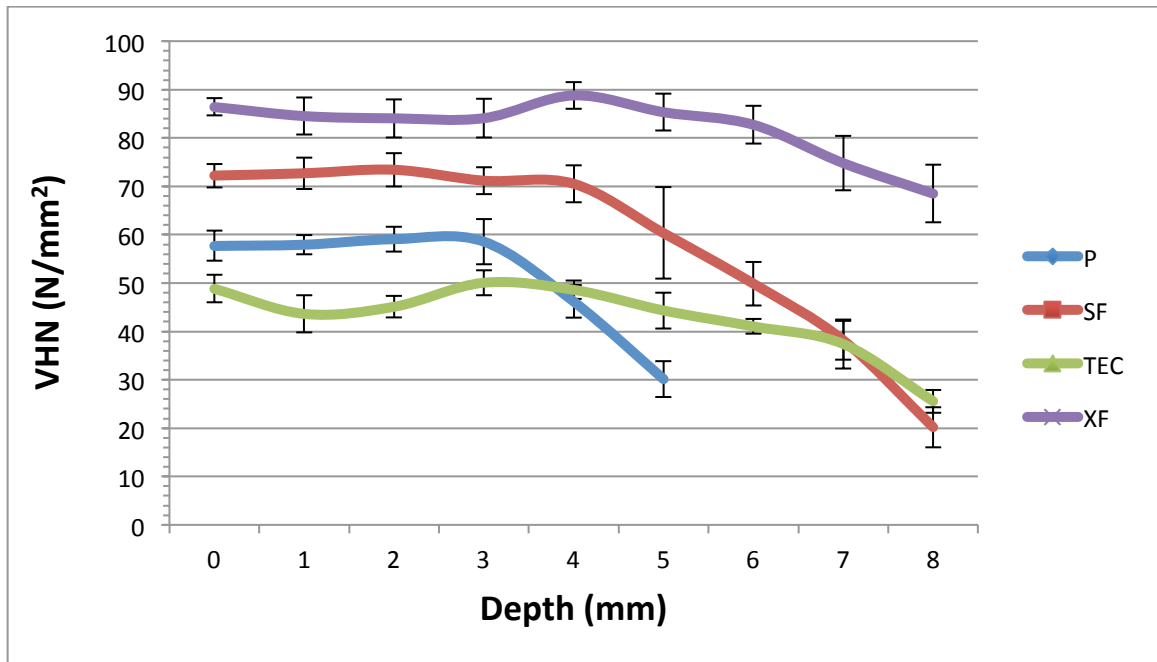


FIGURE 18. Vicker's microhardness (N/mm²) at the top (0 mm) and at the different depths.

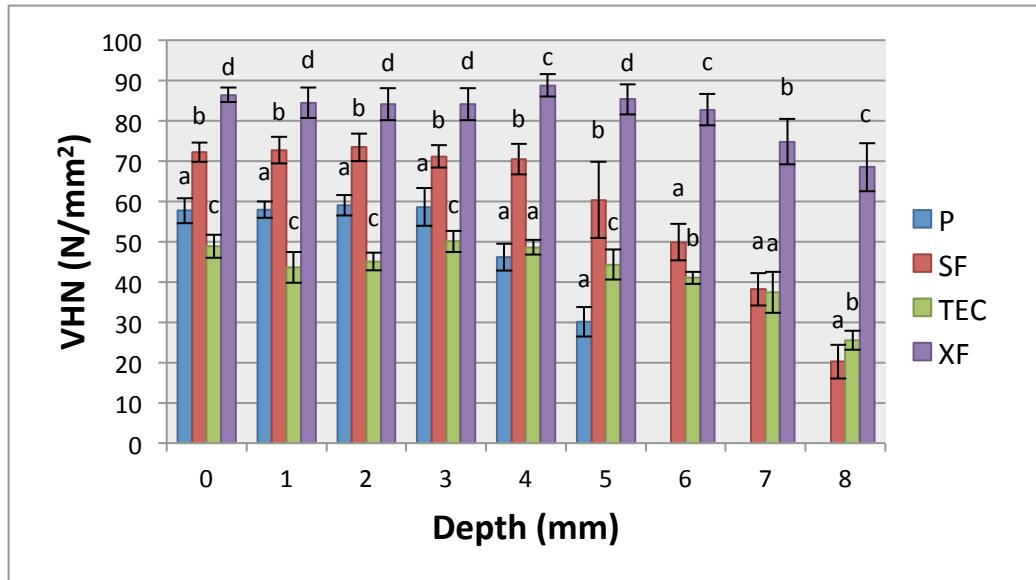


FIGURE 19. Vicker's microhardness (N/mm²) at the top (0 mm) and at the different depths. *Materials with the same letter are not significantly different.

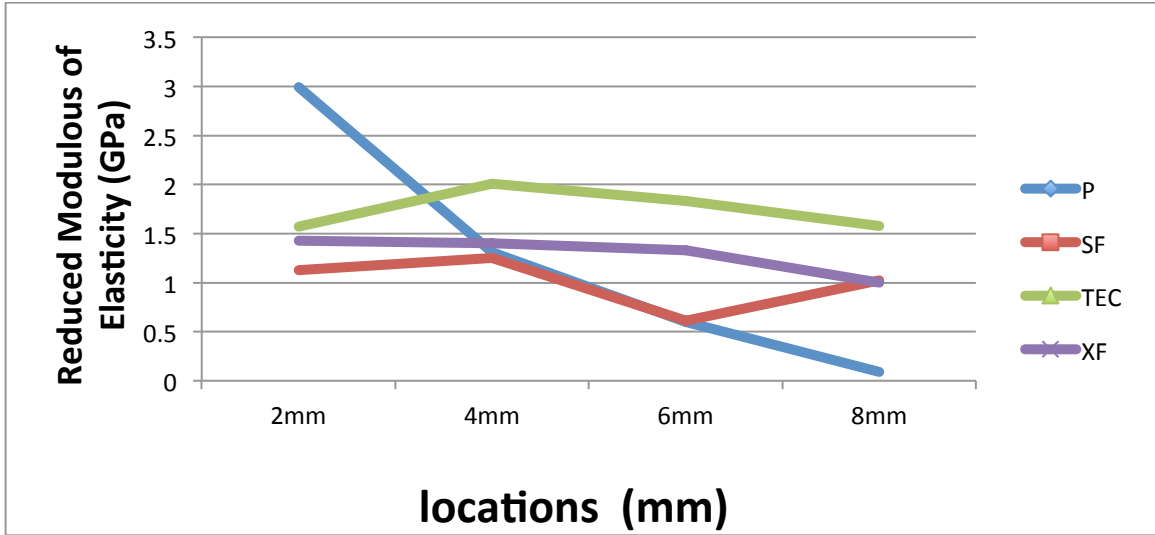


FIGURE 20. Reduced modulus of elasticity (GPa) at four different locations.

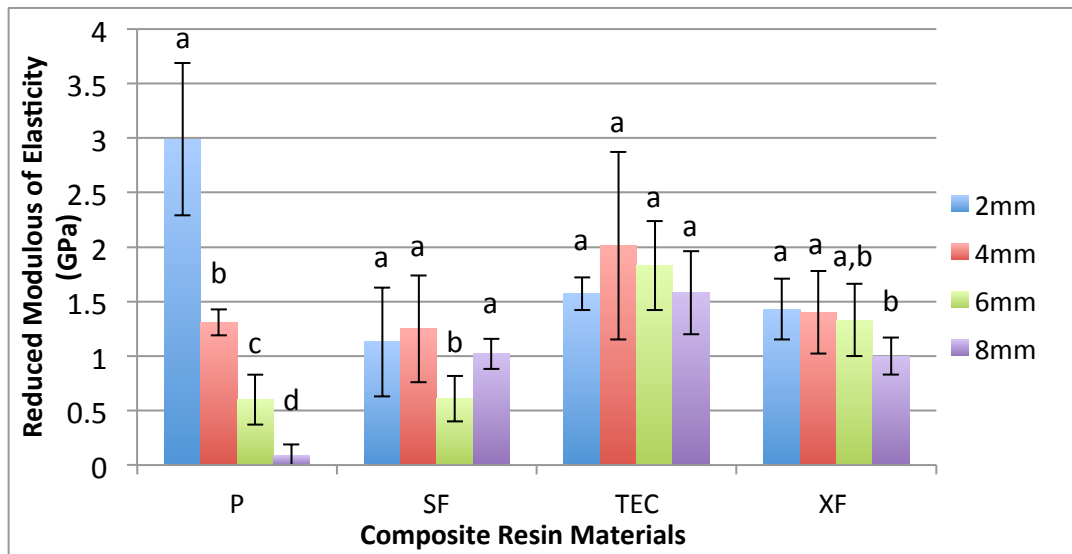


FIGURE 21. Reduced modulus of elasticity (GPa) at four different locations.
*Locations with the same letter are not significantly different.

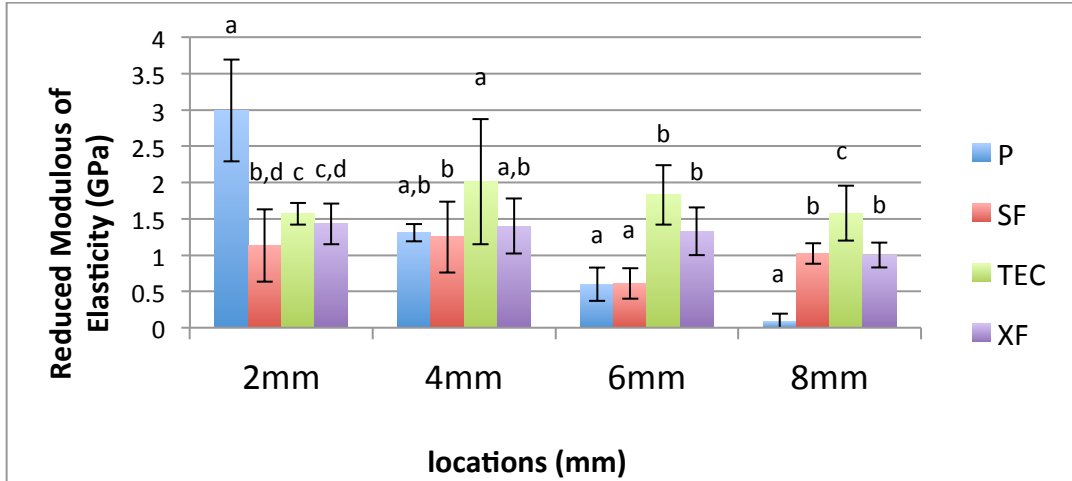


FIGURE 22. Reduced Modulus of elasticity (GPa) at four different locations. *Materials with the same letter are not significantly different.

TABLE I

The composite material used in the study, including information about their type, increment thicknesses, and shades
Light cure protocol for all is ($>500 \text{ mW/cm}^2$, 20 sec)

Product	Manufacturer	Type /consistency	Maximum increment	Shade	LOT-number
Tetric EvoCeram Bulk Fill	Ivoclar Vivadent	Bulk fill /sculptable	4 mm	IVA	S38401
Sonic Fill	Kerr	Bulk Fill Nanohybrid /flowable (sound activated),sculptable	5 mm	A2	5212279
X-tra Fill	VOCO	Bulk fill/Sculptable	4 mm	Universal shade	1506166
Premise	Kerr	Universal Nanofilled /sculptable	2-2.5 mm	A2	5372587

TABLE II

Information about the type of organic matrix and inorganic fillers in each composite material used

Product	Type of organic matrix	Fillers
Tetric EvoCeram Bulk Fill (TEC)	Dimethacrylate	Ba-Glass, YbF ₃ , mixoxide, PPF
Sonic Fill (SF)	TMSPMA, EBPADMA, bisphenol-A-bis-(2 hydroxy-3 methacryloxypropyl) ether, TEGDMA	Glass, oxide, chemicals, SiO ₂
X-tra Fill (XF)	Bis-GMA, UDMA, TEGDMA	-
Premise (P)	EBPADMA, TEGDMA	PPF, Ba-glass, silica fillers

*Data were provided by the manufacturers (missing entries are not specified by the manufacturer). Other abbreviations according to periodic system of elements.⁵²

Abbreviations: Bis-GMA bisphenolglycidylmethacrylate, UDMA urethanedimethacrylate, TEGDMA triethyleneglycoldimethacrylate, TMSPMA 3-trimethoxysilylpropylmethacrylate, EBPADMA ethoxylated bisphenol-A-dimethacrylate, PPF prepolymerized fillers.

TABLE III

The tested depths in each material

Product	Samples Depths (mm)							
	1	2	3	4	5	6	7	8
Tetric EvoCeram Bulk Fill	*	*	*	*	*	*	*	*
Sonic Fill	*	*	*	*	*	*	*	*
X-tra Fill	*	*	*	*	*	*	*	*
Premise	*	*	*	*	*			

TABLE IV

Comparison between the materials in the total energy (J/cm²) transmitted at each depth

Effect: Total Energy Interaction (Material*Depth)								
	1 mm	2 mm	3 mm	4 mm	5 mm	6 mm	7 mm	8 mm
P vs. SF	0.0014	0.2204	0.0189	<0.0001	<0.0001	<0.0001	<0.0001	<0.0001
P vs. TEC	0.0210	<0.0001	<0.0001	<0.0001	<0.0001	<0.0001	<0.0001	<0.0001
P vs. XF	0.0003	<0.0001	<0.0001	<0.0001	<0.0001	<0.0001	<0.0001	<0.0001
SF vs. TEC	<0.0001	<0.0001	<0.0001	<0.0001	<0.0001	0.0001	0.0074	0.0802
SF vs. XF	<0.0001	<0.0001	<0.0001	<0.0001	<0.0001	<0.0001	<0.0001	0.0008
TEC vs. XF	0.1408	0.0544	0.0122	0.0023	0.0016	0.0050	0.0180	0.0451
Conclusion	SF<P<(T EC, X)*	(SF, P)<(TEC, X)	P<SF<T EC<X	P<SF<T EC<X	P<SF<TE C<X	P<SF<T EC<X	P<SF<T EC<X	P<(SF, TEC)<X

TABLE V

Total energy (J/cm²) and mean irradiance (mW/cm²)
at each depth of each composite material

Material	Depth	Total energy J/cm ²	Mean Irradiance mW/cm ²
		Mean (SD)	Mean (SD)
P	1	5.90 (0.21)	289.48 (10.22)
	2	2.26 (0.18)	111.42 (8.94)
	3	0.84 (0.12)	53.72 (3.17)
	4	0.39 (0.04)	19.39 (1.56)
	5	0.09 (0.07)	8.77 (3.62)
SF	1	5.84 (0.40)	285.55 (19.25)
	2	1.97 (0.64)	96.35 (30.74)
	3	1.01 (0.06)	48.88 (3.00)
	4	0.48 (0.04)	23.57 (2.09)
	5	0.31 (0.17)	13.13 (1.28)
	6	0.17(0.06)	10.19(0.87)
	7	0.06 (0.05)	5.93 (5.16)
	8	0.47 (0.14)	12.30 (0.04)
TEC	1	8.42 (0.38)	413.58 (19.17)
	2	4.09 (0.36)	200.92 (17.73)
	3	2.67 (0.14)	131.39 (6.99)
	4	1.49 (0.10)	74.22 (5.29)
	5	0.77 (0.15)	42.20 (4.07)
	6	0.52 (0.02)	25.81 (0.95)
	7	0.34 (0.03)	17.66 (1.32)
	8	0.20 (0.07)	12.18 (1.50)
XF	1	9.15 (0.27)	448.28 (13.22)
	2	5.17 (0.24)	253.70 (12.07)
	3	3.02 (0.15)	147.45 (7.60)
	4	1.91 (0.12)	90.03 (10.70)
	5	1.17 (0.16)	57.18 (7.73)
	6	0.76 (0.13)	38.78 (4.64)
	7	0.56 (0.02)	27.56 (0.75)
	8	0.34 (0.05)	17.46 (2.32)

*Highlighted rows: The depths at which VHN = at least 80 percent of its surface value.

TABLE VI

Vicker's microhardness number VHN (\pm SD) at the top and at each depth

Depth (mm)	Materials			
	Premise	Sonic Fill	TEC	Xrta
Top	57.69(3.1)	72.22(2.44)	48.86(2.89)	86.44(1.76)
1	57.93 (2.00)	72.7(3.27)	43.63(3.87)	84.53(3.81)
2	59.07(2.56)	73.43(3.47)	45.1(2.2)	84.07(3.97)
3	58.57(4.68)	71.17(2.84)	50.07(2.64)	84.1(4.00)
4	46.17 (3.37)	70.53(3.82)	48.6(1.87)	88.8(2.76)
5	30.13 (3.72)	60.33(9.46)	44.33(3.73)	85.33(3.78)
6		49.87(4.52)	41.03(1.5)	82.73(3.91)
7		38.17(4.01)	37.4(5.07)	74.8(5.63)
8		20.2(4.16)	25.57(2.39)	68.5(5.98)

TABLE VII

General comparison between the different materials in regards to their VHN.

Effect	Comparison	p-value	
Material	Premise vs. Sonic	<0.0001	Premise < Sonic < Tetric < X-tra
	Premise vs. Tetric	<0.0001	
	Premise vs. X-tra	<0.0001	
	Sonic vs. Tetric	<0.0001	
	Sonic vs. X-tra	<0.0001	
	Tetric vs. X-tra	<0.0001	

TABLE VIII

The top/bottom ratio of the VHN of each material
(continued on next page)

NEW: VHN Ratio Basic Statistics					
Material	Depth	Min	Max	Mean (SD)	Mean (SE)
Premise	1	0.949153	1.657143	1.11 (0.17)	1.11 (0.03)
	2	0.927273	1.166667	1.05 (0.06)	1.05 (0.01)
	3	0.822581	1.12766	0.96 (0.08)	0.96 (0.01)
	4	0.68254	0.881356	0.78 (0.05)	0.78 (0.01)
	5	0.385965	0.590164	0.51 (0.06)	0.51 (0.01)
Sonic	1	0.873418	1.176471	1.02 (0.08)	1.02 (0.01)
	2	0.886076	1.106061	1.02 (0.05)	1.02 (0.01)
	3	0.909091	1.055556	0.97 (0.04)	0.97 (0.01)
	4	0.822785	1.5	1.05 (0.18)	1.05 (0.03)
	5	0.547945	1.333333	0.90 (0.25)	0.90 (0.04)
	6	0.554054	0.805556	0.68 (0.06)	0.68 (0.01)
	7	0.38961	0.589041	0.51 (0.05)	0.51 (0.01)
	8	0.213333	0.432432	0.27 (0.05)	0.27 (0.01)
Tetric	1	0.77551	1.225	1.00 (0.10)	1.00 (0.02)
	2	0.830189	1.162791	0.98 (0.09)	0.98 (0.02)
	3	0.916667	1.238095	1.08 (0.10)	1.08 (0.02)
	4	0.88	1.093023	0.98 (0.05)	0.98 (0.01)
	5	0.702128	1.021739	0.89 (0.07)	0.89 (0.01)
	6	0.740741	0.877551	0.80 (0.03)	0.80 (0.01)
	7	0.561404	1	0.71	0.71 (0.02)

NEW: VHN Ratio Basic Statistics					
Material	Depth	Min	Max	Mean (SD)	Mean (SE)
				(0.11)	
	8	0.384615	0.574468	0.51 (0.05)	0.51 (0.01)
X-tra	1	0.877778	1.116279	0.99 (0.06)	0.99 (0.01)
	2	0.83871	1.260274	0.98 (0.08)	0.98 (0.01)
	3	0.852632	1.075	1.00 (0.06)	1.00 (0.01)
	4	0.93617	1.169014	1.02 (0.05)	1.02 (0.01)
	5	0.921348	1.103896	1.00 (0.05)	1.00 (0.01)
	6	0.851064	1.0625	0.97 (0.06)	0.97 (0.01)
	7	0.689655	1.025	0.86 (0.07)	0.86 (0.01)
	8	0.604938	0.820225	0.76 (0.05)	0.76 (0.01)

* The highlighted depths are the depth where the bottom VHN was at least 80 percent of the top VHN, and that represent the depth of cure using the vicker's microhardness method.

DISCUSSION

The main goal of the present study was to develop a more profound insight about the polymerization of bulk filling RBCs. The method for achieving such a broad goal is to assess the material through several tests, such as measuring the irradiance and total energy transmitted through the thickness of the RBCs at different depths, microhardness measurements, measurements of the organic resin reduced elastic modulus, and from all data collected, evaluating polymerization threshold energy for bulk fill composites. According to the study's results, the null hypotheses were rejected

VHN

There are no standard conditions for VLC RBCs microhardness testing. Consequently, selecting the testing conditions mainly depends on the researcher's evaluation. There are various studies that have reported Vickers microhardness test for VLC RBCs with different indentation loads and times.^{11,26,53-55}

A study by Yoldas et al. 2004, which intended to determine the effect of different loads and dwell times on the Knoop Hardness test, proposed that a 15-sec dwell time could be accepted as a dwell time limit for dental composites.⁵⁶ Similar studies to formulate standardized parameters for microhardness tests on dental composite would be highly beneficial.

The gradual decrease of the VHN with depth increase was very well presented in the literature.^{11,54,57} All materials tested have reached VHN of 80 percent and above when

the curing protocols of manufacturers' instructions were followed, and the depth of cure claimed by the manufacturer was validated, in agreement with other studies.^{26,52}

However, the VHN values showed a range of variation; the VHN values in this study were similar to the finding by Alshali et al. in 2014 in testing both TEC and SF, but lower than values found in other studies.^{26,53,54}

The variation of microhardness values could be attributed to several factors, such as: variations in specimen fabrication, chemical composition, errors in reading diagonal lengths, and the viscoelastic recovery, and variation in test parameter, especially the indentation load.^{58,59} This study had similarities to Alshali et al. in 2014 in regard to specimen fabrication, the shape and the material of the samples, as well as testing parameters (dry storage for 24 hours and 15 seconds dwell time).⁶⁰

Alshali et al. assessed the initial and the post-irradiation microhardness for selected composite materials. The results showed that all materials tested had a significant increase in microhardness after 24 hours of dry storage, with a wide range of increase from 9.1 percent to 100.1 percent.⁶⁰ Similar findings were also observed in another study with a slightly higher VHN values at 37°C compared to 23°C storage.⁶¹ The increase in microhardness was believed to be attributed to a progressive increase in crosslinking in addition to post-irradiation polymerization reaction.⁶⁰

The indentation size effect (ISE) is a phenomenon of the microhardness values and is dependent on the indentation load. It has been observed in several materials.

Shahdad et al. (2007) argued that the ISE effect is linked to the elastic or plastic deformation under the indenter and to the elastic recovery after the indenter is removed.

Accordingly, it is not appropriate to compare microhardness values if they were obtained with different loads of indentation.⁶²

AFM

From our results, it is clear that the profiles of the studied properties varied with depth. All of VHN, E*, irradiance and total energy values showed a gradual decrease in values with increased material depth. However, this decrease in each property measured has shown to have slight variation in reduction profiles. Whereas, the irradiance and the total energy showed a steady gradual decrease, the VHN showed a slight plateau, then a gradual decrease uniformly in all materials. The E* profile showed a range of variation across the tested materials. This might be attributed to variation in the resin matrix composition between the materials, which might have a direct effect on the mechanical properties of each resin matrix.^{50,60} For example, unlike the other tested materials, the resin matrix E* for TEC showed no significant difference among all four locations, which might be attributed to the Ivocerin (benzoyl germanium compound), a new-photo initiator system that absorbs visible light over a broader wavelength range, from 370 nm to 460 nm.²⁶ On the other hand, TEC is the only material that exhibited a slight increase in the resin matrix E* before it decreases again to a value similar to the first location. This could be associated with different factors, such as the variation in the degree of crosslinking as the depth increases, and the heterogeneity of temperature rise with depth increase during the polymerization process.^{11,63}

In a previous study, it was found that the values of E* of the resin matrix that were measured by AFM were in the same range for the first 2 mm, which was around

2Gpa, as a typical BisGMA/TEGDMA unfilled mixture. That information was taken into consideration when choosing the first testing location in the samples.^{11,64}

The rapid decrease in the resin matrix E^* that was presented in the Leprince et al. 2012 study was not observed in the present study. Henceforth, a certain depth could not be chosen as the point where the resin matrix changes from one physical state to another. The wider range of test locations could explain that finding. For example, that rapid decrease could have happened between location 1 and 2. That being said, monitoring the resin matrix E^* change variation compared with other tests dictates finding a DOC measurement method that takes the quality of resin matrix into consideration. For a future work, a smaller range of testing locations should be taken in consideration before any conclusions could be made about whether the AFM is an appropriate method to test the quality of resin matrix in VLC RBCs.

MARC

In agreement with other studies, the light irradiance and total energy were shown to be gradually decreasing with depth increase. It was also shown that the reduction profile for both parameters accompanies a reduction in the material mechanical properties (VHN and resin matrix E^* in the present study).^{52,53}

It was found that Premise (control) conventional composite material showed the lowest transmitted light when compared with the bulk fill material. This could be due to lower translucency of this material when compared with other test materials. Two factors play a major role in the lack of translucency of Premise, including the moderate size of the inorganic filler particles and the heterogeneous distribution.⁵²

In contrast, XF not only showed higher DOC, but also higher VHN values at all depths as well as higher values of transmitted light energy. This seems to be linked not only to its higher translucency, but also to the inorganic filler content. It has larger filler size compared with the other resin tested. Accordingly, the surface between the fillers and the resin organic matrix is reduced, which leads to less light scattering.^{52,53}

The total energy was shown to be at very low levels, almost zero at some points, yet micromechanical values were not reduced to zero. This shows that the polymerization process is not totally dependent on photoinitiation at deeper points, but rather on an adequate propagation of a polymerization process that starts in the upper layers.⁵³

The total energy or radiant exposure (J/cm^2) is often misused as energy density. It is the result of light radiance (mW/cm^2) and irradiation time (s).⁶⁵

Bucuta et al. in 2014 concluded that a microhardness of >80 percent could be achieved at the bottom surface when the light energy measured at the bottom of the sample was more than $0.7 \text{ J}/\text{cm}^2$.⁵² Similarly, Ilie et al. in 2014 suggested certain values of total energy as a minimum limit of total energy at the top surface to obtain an adequate polymerization at 4 mm of depth.⁵³

This has been a controversial issue. Many studies have stated that it is considered the main factor of determining material properties.²⁹ Established by these studies, exposure reciprocity law declares that similar material properties can be achieved with constant radiant exposure. This suggests the use of high-power illumination can reduce curing time. Many other studies have shown strong opposition to this general rule. The contradicting works state an increase in mechanical properties saturates above a desired radiant exposure. In addition, the DC, flexural strength, flexural modulus, and depth of

cure increase at higher radiant exposure. Ultimately, differing lengths of time and irradiance combinations can lead to substantial differences in material properties.⁶⁶ This is further clarified by the likelihood of loss of radical growth centers by bimolecular termination during polymerization in which the system mobility is elevated. The early termination is more for higher irradiance protocols, due to low conversion termination being equal to the squared concentration of free radicals.²⁹

Polymerization efficiency is closely related to internal factors and affects the applicability of the exposure reciprocity law.³³ There have been enormous differences in DC (44 percent to 72 percent) recorded between constant radiant exposures in a 50/50 wt% of bis-GMA/TEGDMA unfilled resin. In contrast, there were significantly smaller differences (51 percent to 58 percent) with the filling of the same resins. Comparable results have been observed in unfilled resins with increased viscosity and reciprocity holds at >0/40 wt% bis-GMA/TEGDMA ratios, but less viscous resins have shown large differences in DC.

In conclusion, while exposure reciprocity law is upheld for some materials or properties and not in others, it cannot be considered a general rule for all. This becomes more significant due to manufacturers not revealing precise compositions of commercial resin composites. Also, when comparing the composition of conventional composites and flowable counterparts, the unknowns in either co-monomer composition, filler content, and/or photoinitiators can lead to significantly lower DC for high irradiance curing parameters.⁶⁷ Since the majority of studies are conducted with a single irradiation protocol, it is difficult to conclude that these arrangements lead to improved properties.

This means it is applicable for testing all composite innovations or advances to a wide array of irradiances and irradiation times.²⁹

SUMMARY AND CONCLUSION

The AFM method is promising to evaluate the quality of cure of composite resin matrix; however, more research should be done to establish a standardized protocol.

When the manufacturer's instructions were followed, the proposed depth of cure for the bulk fill resin was met.

It is advisable to test all composite innovations or advances to a wide array of irradiances and irradiation times.

REFERENCES

1. Sadowsky SJ. An overview of treatment considerations for esthetic restorations: a review of the literature. *J Prosthet Dent* 2006;96(6):433-42.
2. Kwon Y, Ferracane J, Lee IB. Effect of layering methods, composite type, and flowable liner on the polymerization shrinkage stress of light cured composites. *Dent Mater* 2012;28(7):801-9.
3. Burgess JO, Walker R, Davidson JM. Posterior resin-based composite: review of the literature. *Pediatr Dent* 2002;24(5):465-79.
4. Cramer NB, Stansbury JW, Bowman CN. Recent advances and developments in composite dental restorative materials. *J Dent Res* 2011;90(4):402-16.
5. Powers JM, Sakaguchi RL, Craig RG. *Craig's restorative dental materials*. 12th ed. St. Louis, Mo.:Mosby Elsevier; 2006.
6. Caughman WF, Rueggeberg FA, Curtis JW, Jr. Clinical guidelines for photocuring restorative resins. *J Am Dent Assoc* 1995;126(9):1280-2, 1284, 1286.
7. Rueggeberg FA, Caughman WF, Curtis JW, Jr. Effect of light intensity and exposure duration on cure of resin composite. *Oper Dent* 1994;19(1):26-32.
8. ISOStandards. Polymer based filling, restoration and luting materials. International Organization for Standardization. 2009:1-28.
9. Moore BK, Platt JA, Borges G, Chu TM, Katsilieri I. Depth of cure of dental resin composites: ISO 4049 depth and microhardness of types of materials and shades. *Oper Dent* 2008;33(4):408-12.
10. Bouschlicher MR, Rueggeberg FA, Wilson BM. Correlation of bottom-to-top surface microhardness and conversion ratios for a variety of resin composite compositions. *Oper Dent* 2004;29(6):698-704.
11. Leprince JG, Leveque P, Nysten B, Gallez B, Devaux J, Leloup G. New insight into the "depth of cure" of dimethacrylate-based dental composites. *Dent Mater* 2012;28(5):512-20.
12. Endo T, Finger WJ, Kanehira M, Utterodt A, Komatsu M. Surface texture and roughness of polished nanofill and nanohybrid resin composites. *Dent Mater* 2010;29(2):213-23.
13. Ferracane JL. Elution of leachable components from composites. *J Oral Rehabil* 1994;21(4):441-52.

14. Pearson GJ, Longman CM. Water sorption and solubility of resin-based materials following inadequate polymerization by a visible-light curing system. *J Oral Rehabil* 1989;16(1):57-61.
15. Deliperi S, Bardwell DN. An alternative method to reduce polymerization shrinkage in direct posterior composite restorations. *J Am Dent Assoc* 2002;133(10):1387-98.
16. Lee MR, Cho BH, Son HH, Um CM, Lee IB. Influence of cavity dimension and restoration methods on the cusp deflection of premolars in composite restoration. *Dent Mater* 2007;23(3):288-95.
17. Park J, Chang J, Ferracane J, Lee IB. How should composite be layered to reduce shrinkage stress: incremental or bulk filling? *Dent Mater* 2008;24(11):1501-5.
18. Flury S, Hayoz S, Peutzfeldt A, Husler J, Lussi A. Depth of cure of resin composites: is the ISO 4049 method suitable for bulk fill materials? *Dent Mater* 2012;28(5):521-8.
19. Ilie N, Bucuta S, Draenert M. Bulk-fill resin-based composites: An in vitro assessment of their mechanical performance. *Oper Dent* 2013.
20. Santini A. Current status of visible light activation units and the curing of light-activated resin-based composite materials. *Dent Update* 2010;37(4):214-6, 218-220, 223-217.
21. Ferracane JL. Resin composite--state of the art. *Dent Mater* 2011;27(1):29-38.
22. Mishra MK, Yagci Y, Mishra MK. *Handbook of vinyl polymers: radical polymerization, process, and technology*. 2nd ed. Boca Raton: CRC Press/Taylor & Francis; 2009.
23. Tantbirojn D, Pfeifer CS, Braga RR, Versluis A. Do low-shrink composites reduce polymerization shrinkage effects? *J Dent Res* 2011;90(5):596-601.
24. Li X, Pongprueksa P, Van Meerbeek B, De Munck J. Curing profile of bulk-fill resin-based composites. *J Dent* 2015;43(6):664-72.
25. El-Safty S, Silikas N, Watts DC. Creep deformation of restorative resin-composites intended for bulk-fill placement. *Dent Mater* 2012;28(8):928-35.
26. Alrahlah A, Silikas N, Watts DC. Post-cure depth of cure of bulk fill dental resin-composites. *Dent Mater* 2014;30(2):149-54.

27. Goracci C, Cadenaro M, Fontanive L, et al. Polymerization efficiency and flexural strength of low-stress restorative composites. *Dent Mater* 2014;30(6):688-94.
28. Garoushi S, Sailynoja E, Vallittu PK, Lassila L. Physical properties and depth of cure of a new short fiber reinforced composite. *Dent Mater* 2013;29(8):835-41.
29. Leprince JG, Palin WM, Hadis MA, Devaux J, Leloup G. Progress in dimethacrylate-based dental composite technology and curing efficiency. *Dent Mater* 2013;29(2):139-56.
30. Sakaguchi RL, Powers JM. *Craig's restorative dental materials*. 13th ed. Philadelphia: Elsevier/Mosby;2012.
31. Lovell LG, Newman SM, Bowman CN. The effects of light intensity, temperature, and comonomer composition on the polymerization behavior of dimethacrylate dental resins. *J Dent Res* 1999;78(8):1469-76.
32. Garoushi S, Vallittu PK, Watts DC, Lassila LV. Effect of nanofiller fractions and temperature on polymerization shrinkage on glass fiber reinforced filling material. *Dent Mater* 2008;24(5):606-10.
33. Leprince JG, Hadis M, Shortall AC, et al. Photoinitiator type and applicability of exposure reciprocity law in filled and unfilled photoactive resins. *Dent Mater* 2011;27(2):157-64.
34. Halvorson RH, Erickson RL, Davidson CL. The effect of filler and silane content on conversion of resin-based composite. *Dent Mater* 2003;19(4):327-33.
35. Turssi CP, Ferracane JL, Vogel K. Filler features and their effects on wear and degree of conversion of particulate dental resin composites. *Biomaterials* 2005;26(24):4932-7.
36. Beun S, Bailly C, Dabin A, Vreven J, Devaux J, Leloup G. Rheological properties of experimental Bis-GMA/TEGDMA flowable resin composites with various macrofiller/microfiller ratio. *Dent Mater* 2009;25(2):198-205.
37. Palin WM, Senyilmaz DP, Marquis PM, Shortall AC. Cure width potential for MOD resin composite molar restorations. *Dent Mater* 2008;24(8):1083-94.
38. Moszner N, Fischer UK, Ganster B, Liska R, Rheinberger V. Benzoyl germanium derivatives as novel visible light photoinitiators for dental materials. *Dent Mater* 2008;24(7):901-7.

39. Uhl A, Mills RW, Jandt KD. Photoinitiator dependent composite depth of cure and Knoop hardness with halogen and LED light curing units. *Biomaterials* 2003;24(10):1787-95.
40. Shortall AC, Palin WM, Burtscher P. Refractive index mismatch and monomer reactivity influence composite curing depth. *J Dent Res* 2008;87(1):84-8.
41. Lindberg A, Peutzfeldt A, van Dijken JW. Effect of power density of curing unit, exposure duration, and light guide distance on composite depth of cure. *Clin Oral Investig* 2005;9(2):71-6.
42. Beun S, Glorieux T, Devaux J, Vreven J, Leloup G. Characterization of nanofilled compared to universal and microfilled composites. *Dent Mater* 2007;23(1):51-9.
43. Leprince J, Palin WM, Mullier T, Devaux J, Vreven J, Leloup G. Investigating filler morphology and mechanical properties of new low-shrinkage resin composite types. *J Oral Rehabil* 2010;37(5):364-76.
44. Williams BA, Dickenson DR, Beatch GN. Kinetics of rate-dependent shortening of action potential duration in guinea-pig ventricle; effects of IK1 and IKr blockade. *Br J Pharmacol* 1999;126(6):1426-36.
45. Leprince JG, Palin WM, Vanacker J, Sabbagh J, Devaux J, Leloup G. Physico-mechanical characteristics of commercially available bulk-fill composites. *J Dent* 2014;42(8):993-1000.
46. Alshali RZ, Silikas N, Satterthwaite JD. Degree of conversion of bulk-fill compared to conventional resin-composites at two time intervals. *Dent Mater* 2013;29(9):e213-217.
47. Tiba A, Zeller GG, Estrich CG, Hong A. A laboratory evaluation of bulk-fill versus traditional multi-increment-fill resin-based composites. *J Am Dent Assoc* 2013;144(10):1182-3.
48. Kwon TY, Bagheri R, Kim YK, Kim KH, Burrow MF. Cure mechanisms in materials for use in esthetic dentistry. *J Investig Clin Dent* 2012;3(1):3-16.
49. Rueggeberg F. Contemporary issues in photocuring. *Compend Contin Educ Dent Suppl.* 1999(25):S4-15; quiz S73.
50. Alshali RZ, Salim NA, Sung R, Satterthwaite JD, Silikas N. Qualitative and quantitative characterization of monomers of uncured bulk-fill and conventional resin-composites using liquid chromatography/mass spectrometry. *Dent Mater* 2015;31(6):711-20.

51. Arika D. Kemp CCH, Wayne A. Cabral , Joan C. Marini , Joseph M. Wallace Effects of tissue hydration on nanoscale structural morphology and mechanics of individual Type I collagen fibrils in the Brtl mouse model of Osteogenesis Imperfecta. *J Structural Biol* 2012;180:428–38.
52. Bucuta S, Ilie N. Light transmittance and micro-mechanical properties of bulk fill vs. conventional resin based composites. *Clin Oral Investig* 2014;18(8):1991-2000.
53. Ilie N, Stark K. Curing behaviour of high-viscosity bulk-fill composites. *J Dent* 2014;42(8):977-85.
54. Flury S, Peutzfeldt A, Lussi A. Influence of increment thickness on microhardness and dentin bond strength of bulk fill resin composites. *Dent Mater* 2014;30(10):1104-12.
55. Ilie N, Bucuta S, Draenert M. Bulk-fill resin-based composites: an in vitro assessment of their mechanical performance. *Oper Dent* 2013;38(6):618-25.
56. Oguz yoldas TA, Hakan Uysal Influence of different indentation loads and Dwell time on Knoop Microhardness tests for composite material *Polymer Testing* 2004;23:343-6.
57. Alrahlah A, Silikas N, Watts DC. Hygroscopic expansion kinetics of dental resin-composites. *Dent Mater* 2014;30(2):143-8.
58. Sangwal k sB, Blaziak p analysis of indentation size effect in microhardness measurement of some cobalt -based alloys. *Material Chemistry Physics* 2003;77(2):511-20.
59. Chanya chuenarrom pb, paitoon daosodasi. Effect of indentation load and time on knoop and vickers microhardness tests for enamel and dentin. *Material Res* 2009;12(4):473-6.
60. Alshali RZ, Salim NA, Satterthwaite JD, Silikas N. Post-irradiation hardness development, chemical softening, and thermal stability of bulk-fill and conventional resin-composites. *J Dent Feb* 2015;43(2):209-18.
61. Watts DC, Amer OM, Combe EC. Surface hardness development in light-cured composites. *Dent Mater* 1987;3(5):265-9.
62. Shahdad SA, McCabe JF, Bull S, Rusby S, Wassell RW. Hardness measured with traditional Vickers and Martens hardness methods. *Dent Mater* 2007;23(9):1079-85.

63. Asmussen E, Peutzfeldt A. Influence of specimen diameter on the relationship between subsurface depth and hardness of a light-cured resin composite. *Eur J Oral Sci* 2003;111(6):543-6.
64. Sakaguchi RL, Wiltbank BD, Murchison CF. Prediction of composite elastic modulus and polymerization shrinkage by computational micromechanics. *Dent Mater* 2004;20(4):397-401.
65. Kirkpatrick SJ. A primer on radiometry. *Dent Mater* 2005;21(1):21-6.
66. Peutzfeldt A, Asmussen E. Resin composite properties and energy density of light cure. *J Dent Res* 2005;84(7):659-62.
67. Hadis M, Leprince JG, Shortall AC, Devaux J, Leloup G, Palin WM. High irradiance curing and anomalies of exposure reciprocity law in resin-based materials. *J Dent* 2011;39(8):549-57.

ABSTRACT

IN VITRO EVALUATION OF POLYMERIZATION ENERGY FOR
BULK FILL COMPOSITES

by

Rawan S. AlRasheed

Indiana University School of Dentistry
Indianapolis, Indiana

Recently, the concept of “bulk-fill” resin-based composites (RBCs) has been re-emphasized, with claimed improvements in depth of cure (DOC) with similar mechanical properties and comparable adaptation to walls and margins relative to conventional composite. More research is needed to carefully examine the properties of these new materials. The objective of this study was to measure the light energy, microhardness

(VHN), and elastic modulus across the depth of one conventional and three bulk-fill RBCs.

Materials and Methods: Three commercially available bulk-fill RBCs (Tetric EvoCeram Bulk Fill [TE], SonicFill [SF], X-tra fill[XF]) and one conventional RBC (Premise [PR]) were evaluated (n = 10). DOC (using Vickers's microhardness), elastic modulus (using atomic force microscopy), and the mean irradiance and total light energy transmitted through different thicknesses of RBC were measured by a spectrometer. The effects of group, location, and curing depth on VHN were analyzed using mixed-model ANOVA. Elastic modulus and light energy comparisons were made using two-way ANOVA, with a significance level of 5 percent.

Results: There was a significant difference in the depths for the mean irradiance and total energy between different depths in all materials. All materials achieved the manufacturers' claimed DOC. XF had the highest DOC with 7 mm and a light energy of 0.56 ± 0.02 J/cm² at 7 mm. PR had the lowest DOC with 3 mm and a light energy of 0.84 ± 0.12 J/cm² at 3 mm. The elastic modulus showed significant variation in depth profiles that were different than the DOC.

Significance: The manufacturers' claims for bulk-fill DOC were achieved using a microhardness method. However, this method failed to detect the quality of the polymerization. Assessment of the elastic modulus using AFM is a promising method for greater understanding of the polymerization.

CURRICULUM VITAE

Rawan Saleh AlRasheed

October 1985	Born in Riyadh, Saudi Arabia
July 2004	AlRowad Private School for girls Riyadh, Saudi Arabia
July 2009	Bachelor of Dental Surgery (BDS), King Saud University Riyadh, Saudi Arabia
July 2009 to July 2010	Internship – General Dentistry King Saud University Military Hospital in Riyadh
August 2010	Teaching Assistant King Saud University
August 2014	Accepted in Doctoral Program, Indiana University, School of dentistry Indianapolis, IN
May 2016	MSD, Operative Dentistry, Indiana University School of Dentistry, Indianapolis, IN